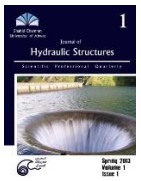
Journal of Hydraulic Structures
***J. Hydraul. Struct.*, 2016; 2(1):12-26**
DOI: 10.22055/jhs.2016.12647



Experimental Investigation of Rill Creating Hydraulic Conditions in the Marl Rangelands in a Tilting Flume

Amin Zoratipour[1]
Hossein Azadi[2]

Abstract

Generally, the evaluation and assessment of the critical condition of rill formation are useful for a better understanding of soil erosion processes. The inherence characteristics of soils, which have much dynamic variations on the hillslopes and are affected by rill formation, are the soil critical shear stress and soil erodibility factors. This study aims to assess experimental rill incision thresholds, the determined soil critical shear and soil erodibility factors on marl formation based on precipitation characteristics and different slope gradients on sensitive marl soil. The results showed that the rainfall intensity and slope steepness factors separately and together can significantly affect the distance from the point of rill initiation; runoff and rill start time and soil loss values. Rainfall intensity showed more importance than the slope gradient in the point of rill formation. There is a significant relationship between rainfall intensity and slope gradient with rill incision point, time of runoff start and rill start and soil loss. The point of rills formation (slope length) decreases with an increase in slope gradient and rainfall intensity. Finally, the results revealed that the values of soil erodibility factor (Kr) and critical shear stress of marl soil are 0.0015s m^{-1} and 0.267N m^{-2}, respectively.

Keywords: Critical shear stress, soil erosion rate, rainfall intensity, slope gradient, marl

Received: 25 December 2015; Accepted: 15 April 2016

1. Introduction

Most of previous studies show that rain-impacted flows are largely responsible for erosion in rill and interrill erosion areas (Kinnell, 2005). Generally, the mechanisms of soil erosion by splash, interrill and rill erosion are water erosion sub-processes which have different mechanisms (Govers et al., 1986). Interrill erosion and rill erosion are the two basic types of soil erosion in agricultural catchments in Iran. When a rainstorm event occurs, both commonly coexist on steep slopes,

[1] Assistant Professor, Ramin Agriculture and Natural Resources Uni., zoratipor@yahoo.com (**Corresponding author**)
[2]Assistant Professor, Scientific Staff of Gent Uni.

especially in the marl areas of Iran. The rill formation process includes three stages: detachment, entrainment, and the transport of soil particles driven by concentrated surface water. Rill erosion is the second stage of the erosion dynamic process in catchments, which is a function of soil erodibility factor, soil hydraulic transfer capacity and flow shear stress (Kinnell et al., 2005). Rills are characterized as an incised channel that is at least 5 cm length, 0.5 cm deep, and 1 to 2 cm wide (Torri et al., 1987). After creation, the rills expanded the upstream and downstream of hill-slopes (Toy et al., 2002). According to Horton's (1945) threshold theory, the rate at which soil particles are detached can be related to the amount by which one of the flow hydraulics variables such as flow stress shear, stream power and unit discharge, characterizing the hydraulics of the flow, exceeds a critical soil specific value (Knapen et al., 2007). Some studies indicate that soil erosion resistance to the concentrated flow is influenced by almost any soil property. In other words, rill incision begins when overland flow shear stress exceeds soil critical shear stress. Obviously, the expanding of rills depends on some parameters such as water shear force (flow shear stress) and soil resistance. Therefore, soil erosion made by the concentrated flow is highly dependent on flow conditions and soil interior characteristics such as critical shear stress. When the overland flow reaches a critical point (the point at which soil particles lose the ability to remain in place and are detached by flowing water), a rill starts to form. Although studies (Romero et al., 2007; Zhang et al., 2008) on concentrated flows and rill formation processes have mainly focused on small plots, and only a single rill; studies with larger plots that allow observations of groups of rills would lead to more generalized conclusions are rill initially being formed on a hillslope (Toy et al., 2002). Yao et al., (2008) carried out a study related to the critical shear stress on an eroding rill to slope steepness and discharge on silty-clay soil from the Loess Plateau in China in a large sloping indoor plot (8m×3m) with five different slope gradients using simulated rainfall at three rainfall intensities. He observed that slope was rather more important than rainfall intensity in determining the location of the rill initiation. The range of soil critical shear stress in his study was determined from 1.33 to 2.63 Pa. The soil critical shear stress was also inversely related to the slope gradient and not influenced by the rainfall intensity.

Generally, the marl formation field is one of the important sensitive soils to rill and gully erosions and also is the most sediment resource in the Iran that gives a high priority to be studied (Ahmadi, 1999). Given only few studies have been conducted on knowing the dynamic variations of rill erosion in marl degraded lands in general, and especially in Iran, the general goal of this study is to realize the dynamic variations of rill erosion degraded rangelands on marl in the country. Considering the lack of temporal and spatial reliable quantitative information in the scale of each rill, the study assesses the temporal and spatial thresholds of rill formation and soil loss values in marl degraded rangelands of Iran. Furthermore, the study estimates the critical shear stress and soil erodibility factors in the laboratory flume.

2. Material and methods

Study area

The study was carried out in the Taleghan watershed, a midstream tributary of the Sefid Roud basin in the north of Iran (Fig. 1). The watershed is located between 36° 5′ 17″ and 36° 20′ 45″ N and 50° 39′ 33″ and 51° 11′ 26″ E, and ranges in elevation from 1852 to 4100 m. According to the FAO (1993) classification, the climate is semi-arid and the average annual precipitation at the Taleghan station is 480 mm. The total area of the basin is 1243km^2.

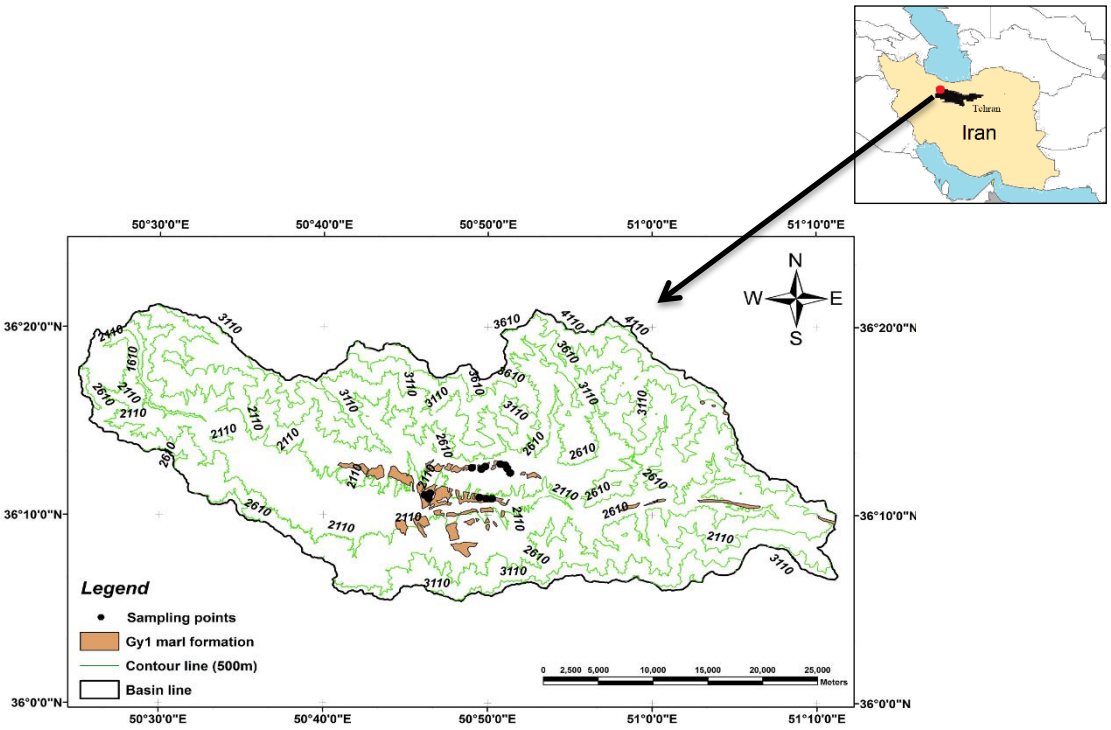


Fig.1.The location of the Taleghan watershed in Iran and the location of sampled points of the marl formation

Marl formations and marl sub-layers cover about 25-30 million ha of Iran's area (Soil Conservation and Watershed Management Research Center of Iran, 2005). The saline-gypsum marl formations cover a wide area of lands in arid and semi-arid regions of Iran. Marl formation consists of different classes on the base physical and chemical properties soil particles, which includes: Ngc, Ngm, Gy_1 and Gy_2 marls (Ahmadi, 2006). According to some studies (Ahmadi, 1999), the Gy_1 and Gy_2 marl formations, due to the presence of gypsum and salt materials, are more erodible than rest of marl formations, as the thickness of this formation is estimated approximately 200-300 meters. These formations are one of the greatest sources of the country's sediment, with a high degree of erodibility. In away Gy_1 saline-gypsum formation has decreased the effective longevity of huge dams in Iran such as Sefidroud and Taleghan Glinak (Ahmadi, 2006). Erosion processes in this kind of marl are active and include different forms of erosion such as, interrill, sheet, rill, gully, piping and badland formation. It should be noted that the vegetation cover at marl areas is low and it has a sparse distribution (Ahmadi, 1999) that shows the rill and interrill erosion in degraded rangelands of the Taleghan watershed are common (Fig. 2). Table 1 shows that the soil of the case study has a clay texture. It also shows the physical and chemical properties of the marl soil in different points (12 points) of the Taleghan basin.



Fig.2.Rill and interrill area in degraded lands of the Taleghan basin

Table 1.The average of some physical and chemical properties* of the marl soil of the study area used in the rainfall-erosion simulate

Characteristic	*Average*	*S.d. (±)***	*Characteristic*	*Average*	*S.d. (±)*
Sand	*6%*	*1.7*	*pH*	*7.9*	*0.05*
Silt	*38%*	*3.3*	*EC*	*0.26(dS m^{-1})*	*0.01*
Clay	*56%*	*2.9*	*Gypsum*	*11.3%*	*1.7*
Bulk density	*1.4(g cm^{-3})*	*0.03*	*$CaCo_3$*	*19.2%*	*2.1*
Porosity	*46.2%*	*4.9*	*Saturation*	*42.2%*	*4.2*
Organic matter content	*0.45%*	*0.13*	*Stones and pebbles*	*8.5%*	*2.5*

* The soil texture was defined by USDA (1991), Bulk density is performed with clod method (Blake and Hartge; 1986), Organic matter content by Nelson and Sommers (1982), EC and pH by Kiniry et al. (1983), Gypsum, CaCo3, Saturation and Porosity by Klute (1986); Page et al. (1982). ***S.d.: Standard deviation.*

Experimental setup

The experiment was conducted in a (1m×6m) tilting flume in the laboratory at the Institute of Soil Conservation and Watershed Management Research, Iran. The flume has advantages such as pressurized water, rainfall plane 7.75 m above the flume level, changeable slope up to 60% and the capability of intensity regulation (10-125 mm/h). At the preparation stage of the experimental flume, after transporting the soil from the field to the experimental site, the soil was air-dried. The clods in the soil were broken up, and the soil was sieved with a 10 mm screen. A 15 cm layer of gravel particles was uniformly placed in the bottom of the plot box as drainage layer. On the top of the gravel layer, a marl soil was packed loosely and evenly by a depth of 25 cm. The soil used in this experiment was obtained from the root layer (50 cm top soil level) of degraded marl rangelands in the Taleghan watershed (Fig.1). A protective thick gauze cloth was located between gravel particles and marl soil surface. During the packing process, a static weight method was used to compact the soil uniformly in the box (Yao et al., 2008). After packing the flume of soil and

compacting it layer by layer with a homogeneous cylinder, the soil surface was smoothed manually with a rake. Then, the plot was prepared in a horizontal position and the flume soil was saturated from the below surface of the flume. After the soil saturation, to let the soil become equilibrated, it was left for at least 24 h, such that the surplus water came out of outlet drainage. Thus, the plot remained in a horizontal position to ensure a uniform and homogeneous initial soil moisture profile (Yao et al., 2008). In the beginning of each experiment, before performing the simulated rainfall, the bulk density test is determined randomly from the compacted soil (superficial and deep samplers), such that the bulk density of the compacted soil complied with the bulk density of field conditions. The same action was performed in other experiments.

Using the curves of rainfall intensity-duration-frequency from the Taleghan Synoptic station, this study first evaluated the rainfall distribution. The distribution was selected of rainfall with return periods of 2, 25, and 100 years. Then, the selected rainfalls were generated and calibrated by the rainfall simulator to simulate the erosion-rainfall process. So, the simulation of erosion-rainfall process at the intensities of 10, 55 and 110 (mm h^{-1}) presents the intensity of rainfall at the return periods of 2, 25 and 100 years, respectively. A large runoff plot (1m×6m) was used with a rainfall simulator (Fig. 3). The plot rested on a platform that was adjustable to two slope gradient (22.17% and 44.63%). To measure the position of the rill initiation during the experiment, the rulers were fixed on the metal borders of the plot, and the entire plot surface was divided into 6 blocks (1 m^2 each). The soil was packed in the plot to a bulk density of 1.4 g cm^{-3} for every layer. The treatments included two slope gradients 22.17% and 46.63%, each with a three-level of rainfall intensity (10, 55, and 110 mm h^{-1}) and they were carried out in two repetitions. These ranges for the slope gradient and rainfall intensity were selected to cover the storm and field conditions observed in the Taleghan basin. In this study, the ranges were selected as erosion critical conditions on the Gy_1 marl formation in Taleghan. Finally, 12 different treatments on the bases of the slope steepness and rainfall intensities were simulated.

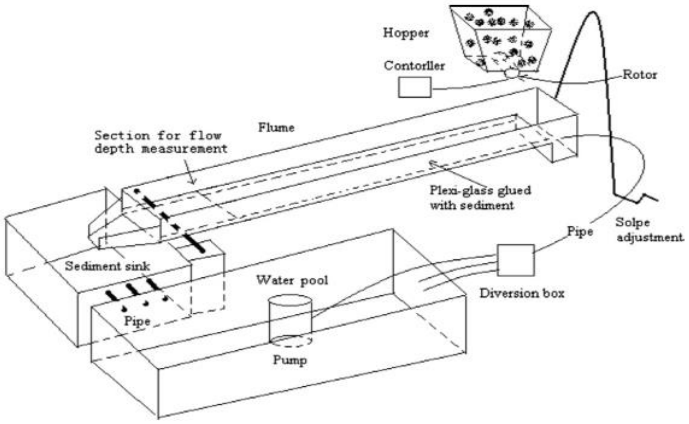


Fig.3. Schematic diagram of experimental set-up of the tilting flume

Experimental Procedure

Following the soil preparation, every experiment was performed 24 h after the initial saturation. At the initial stage of each experiment, the flume was set at the desired slope gradient and rainfall intensity. In each test, the starting time of the simulated rainfall, the time when runoff reached the outlet of the plot, and the time when rill initiation occurred were recorded. In each experiment,

sediment samples together with runoff were taken every minute for about 30 minutes after the start of the runoff. The runoff discharge, runoff volume, and sediment concentration were measured at the outlet of the test plot for different rainfall intensities and slope gradients. During the experiments, the flow velocity was measured by the dye tracing technique (potassium permanganate) and also using a stopwatch to record the time required for the dye to travel a given distance (Yao et al., 2008). The flow velocities were measured by recording the travel time of the dye cloud over a distance of 1 m. The average travel time was taken as the mean of 5 measurements (each 6-minute, one time) (Cao et al., 2009). The runoff samples were allowed to settle overnight to separate the suspended sediments from water in the samples. The remaining water and sediment were transferred into containers that were dried in ovens at 105°C for more than 24h, or until the samples got completely dry. Then, the mass of the sediment was measured and used to calculate the sediment concentration. In addition, the distance from the top of the plot to the point of initiation was measured; the median distance of all rills in a test was used in subsequent calculations as length to the rill initiation (Yao et al., 2008). During each experiment, the distance from the top of the plot to the point of rill initiation, time of runoff start and time of rill start on the soil surface were measured.

Data analysis

According to Cao et al., (2009), the critical conditions of rill incision relates to hydraulic parameters of the surface water flow and soil inherence characteristics. In this regard, Yao et al. (2008) explained that the critical point of rill incision is a small pit that is created on the plot or hillslope during the experiment and then develops into a rill. Accordingly, two important parameters for the rill initiation are considered as the flow shear stress and soil erodibility coefficient. Several approaches are used in different studies to estimate flow hydraulic parameters such as shear stress, stream power and the determination of soil detachment in rills. The hydraulic shear stress; τ (Pa), on the bases equations of simple force-balance for uniform flow depth, can be derived from Cao et al., (2009):

$$\tau = \rho\, g\, h_i\, S \tag{1}$$

where τ (Pa) is the shear stress, ρ (kg m^{-3}) is the water mass density, g (m s^{-2}) is the gravity constant, h (m) is the flow depth, and S is the tangent value of slope gradient. Also, the flow depth at the above equation was calculated by the following equation (Yao et al., 2008):

$$h = \frac{q}{V} \tag{2}$$

where h (m) is the flow mean depth, q (m^2 s^{-1}) is the unit flow discharge at the outlet point and V (m s^{-1}) is the flow mean velocity on the hillslope. Also, the stream power (ω) can be calculated from the equation (3), as Cao et al. (2009):

$$\omega = \tau V = \rho\, g\, h\, S\, V \tag{3}$$

where ω (kg m^{-3}) is the stream power, V (m s^{-1}) is the mean flow velocity. According to Knapen et al. (2007), in the case of predicting soil detachment from simple hydraulic indicators, there are several basic models to predict soil detachment which use the main hydraulic variables that control soil detachments such as slope gradient, flow velocity, flow depth and the hydraulic roughness

factor to the measured soil loss. Different studies have presented the two models according to threshold concept to predict the rill detachment capacity; one is used for the excess shear stress models and the other excess stream power models. In order to predict the rill detachment capacity on the base of excess shear stress model, the general form of this equation is used, as shown in the equation (4) (Govers et al., 2007):

$$D_c = K\,(a\tau - \tau_c)^b \quad (4)$$

where D_c is the amount of sediment detached per unit of bed surface per unit of time (kg m^{-2} s^{-1}), K is soil erodibility factor (s m^{-1}), τ is the shear stress of the flow (N m^{-2}), τ_c is the critical shear stress of soil (N m^{-2}), a and b are constants. It should be mentioned that K, a, b and τ_c are determined empirically. In most cases, the constants a and b are assumed equal to unity or close to unity (e.g., b =1.05) (Govers et al., 2007, p. 89). The rill erosion rate (D_r) per plot could be calculated from the erosion rate per rill, multiplied by the number of rills, and divided by the plot area (Sheridan et al., 2000). Generally, the soil detachment rate is defined as the soil loss of per square meter per second. In this study, the rate was calculated as the total mass of soil loss (original oven-dry mass minus final oven-dry mass) divided by the time interval of the test and the cross-section area of the soil sample (Cao et al., 2009). The following rill detachment equation was applied to calculate K_r values (Romero et al., 2007; Govers, et al., 2007):

$$D_c = K_r\,(\tau - \tau_c) \quad (5)$$

where D_c = rill detachment capacity for clean water (kg m^{-2} s^{-1}); K_r = rill erodibility (s m^{-1}); τ_c = the shear below when there is no detachment or critical shear stress (Pa); τ = hydraulic shear stress of flowing water (Pa); $\tau = \gamma rs$, where γ = specific weight of water = 9810 N m^{-3}; r = hydraulic radius of rill, m; and s = hydraulic gradient of rill flow). In this paper, the rill erodibility parameters K_r and τ_c are determined experimentally from the measured erosion rates at a range of flow shear values. The measured rill detachment values (kg m^{-2} s^{-1}) were plotted against the hydraulic shear (Pa) values. The slope of the regression line is K_r, and the intercept with the horizontal axis is the critical shear, τ_c. Lastly, the critical slope length to the rill initiation is defined as the distance from the top of the plot to the point where a rill began to form which each test was determined (Sheridan et al., 2000; Knapen et al., 2007). Also, in this study, Change Rate factor (Cr) was used to determine sensitive variables in soil erosion between slope steepness and rainfall intensity at different treatments. This factor shows the sensitive analysis quantitatively, i.e. the amount of change in interval to rill incision to the upside of the flume in different slope gradients and rainfall intensities. The general form of this relationship is defined in the equation (6) (Yao et al., 2008):

$$cr = \frac{\Delta L_i}{L_o} \times 100 \quad (6)$$

Where cr is the change rate (%) of interval of rill initiation, ΔL_i is the change range of slope length to the rill incision from one treatment to another, and L_0 is the slope length to rill incision of 22.17% slope gradient in different rainfall intensities or that of 10 mm h^{-1} rainfall intensity in different slopes.

3. Results

Relationships between hydraulic parameters

Table 2, presents the flow unit discharges, flow mean velocity, flow depth, and flow shear stress for each treatment. According to the results of the table, the shear stress can range from 0.217 to 2.075 Pa. Also, the results showed that the increased flow discharge leads to an increase in the flow depth and followed by an increase in the flow shear stresses.

Fig. 4 shows a linear regression between shear stress changes and the rate of rill detachment in all the simulation tests. Thus, the values of marl soil erodibilty factor Gy_1 (K_r) and critical shear stress of marl soil can directly be estimated by using the rainfall simulator (line slope and intercept of the graph represents (Kr) and (τ) values respectively). Finally, according to the results, the values of marl soil erodibilty factor (K_r) and the critical shear stress of marl soil Gy_1 are 0.0015 (s m^{-1}) and 0.267 (N m^{-2}), respectively.

Sensitivity Analysis

The results average of all the observations for a given experiment that was calculated as the slope length to the rill initiation (Figs 5 to 7). In addition, Table 3 shows the results of reaching time of the runoff at the plot outlet as the runoff start threshold, the start time of rill incision as rill formation threshold, and the total amount of soil loss in each treatment. Sensitivity analysis of results shows that the slope length of rill initiation has a greater sensitivity to rainfall intensity than to slope gradient. According to the results of the table 2, the impact of rainfall intensity on the slope length to rill initiation is more significant than that of the slope steepness: 36.1% versus 13.6% within the tested range.

Results of variance analyses and means comparison variables

Variance analysis

To study the significance of the investigated factors on the studied variables, an analysis of variance was performed using SAS software (version 9.1). Table 2 and Figs. 5-7 show the results of variance analyses of different variables, also means comparison in different categories. The results indicate high significant ($P \leq 0.01$) differences for the slope gradient and intensity in all the studied variables (Table 2). Also apart from the rill incision point, the ANOVA estimation showed that the interaction effects between slope and intensity were significant in the rest of variables.

Results of means comparison: Runoff start time and rill start time

The obtained means of the studied factors and their corresponding interaction of each variable were separately subjected to the Tukey test that uses the studentized range statistic to make all of the pairwise comparisons between groups (McHugh et al., 2007). The averages of the runoff start time in the three selected levels of the rainfall intensity (10, 55 and110 mm h^{-1}) were realized differently (Fig. 5a). The lowest intensity significantly shows the highest runoff start time compared to the two others (11'30" vs. 2'30" and 1'25"). Also, the averages of the runoff start time in the two selected levels of the slope gradient (22.17 and 44.63%) were realized dissimilar as

Table2. Hydraulic parameters of rainfall-induced surface flow

Test	*Rainfall intensity (mm/h)*	*Slope gradient (%)*	*Repetition*	*Flow unit discharge (m^2/s)*	*Mean flow velocity (m/s)*	*Mean flow depth ($m\times10^{-3}$)*	*Flow shear stress (N/m^2)*
1	10	22	1	0.0000413	0.073	0. 566	0.2430
2	10	22	2	0.0000365	0.078	0. 467	0.2168
3	10	44	1	0.0001842	0.125	1.473	0.3425
4	10	44	2	0.000241	0.12	2.008	0.4673
5	55	22	1	0.00031	0.143	2.200	1.0379
6	55	22	2	0.00029	0.161	1.809	0.9420
7	55	44	1	0.00112	0.196	5.702	1.6334
8	55	44	2	0.000872	0.191	4.564	1.2286
9	110	22	1	0.000422	0.204	2.066	0.9758
10	110	22	2	0.000495	0.203	2.442	1.1587
11	110	44	1	0.002337	0.27	8.653	2.0745
12	110	44	2	0.0017	0.29	5.843	1.4174

Table3. Results of variance analysis of the variables Runoff start time, Rill start time, Rill incision point and soil loss between treatments

	Runoff start time	***Rill start time***	***Rill incision point***	***Soil loss***
	M.S	***M.S***	***M.S***	***M.S***
Slope gradient	*38.9***	*25.23***	*0.65**	*1.055***
Rain fall intensity	*123.3***	*125.26***	*5.9***	*18.57***
Interaction	*28.83***	*12.93**	*0.243^{ns}*	*0.83***
CV%	*18.8*	*18.16*	*6.1*	*12.94*

** Significant at the level of 0.05($P \leq 0.05$) ** Significant at the level of 0.01 ($P \leq 0.01$), ns, nor significant, M.S.: mean squares*

shown in Fig. 5b. The lowest slope significantly shows the highest runoff start time compared to the other (6'35" vs. 3'20"). Furthermore, the interaction effects of the two factors (rainfall intensity

and slope gradient) were estimated in Fig. 5c. As shown in the figure, the averages of the runoff start time in the lowest intensity are significantly different compared to the two others in the slope level of 22% (16' 25" vs. 2' 45" and 1'40" respectively). According to the figure, the averages of the runoff start time in the other slope level (44%) are similar to the slope gradient 22% in the three rainfall intensities (6' 40" vs. 2' 15" and 1'15" respectively).

Also for the variable rill start time (in the same figure), the averages of the rill start time of the three selected levels of the rainfall intensity (10, 55 and110 mm h^{-1}) were recognized dissimilar (Fig. 5a). The lowest intensity significantly shows the highest rill start time compared to the two others (12'35" vs. 4'15" and 1'25"). Furthermore, the averages of the rill start time of the two selected levels of the slope gradients (22 and 44%) were recognized differently (Fig. 5b). The lowest slope gradient significantly shows the highest rill start time compared to the other (7'40" vs. 4'45"). Also, the interaction effects of the two factors (rainfall intensity and slope) in Fig. 4c shows that the averages of the rill start time are significantly different in the slope level of 22% in the three rainfall intensities (16'5", 4'45" and 2'15"). According to the figure, the averages of the rill start time in the other slope level (44%) in the lowest intensity are significantly different compared to the two others (9'00" vs. 3'45" and 1'30"). Consequently, the lowest levels of both intensity show the highest rill start time (16'5" in 10 mm h^{-1} and 9'00" in 110 mm h^{-1}). In other words, the highest levels of intensity show the lowest rill start time (Fig. 5c).

Results of means comparison: Rill incision point

With regards to the variable rill incision point, according to Fig. 6a, the averages of the rill incision point in the three selected levels of the rainfall intensity (10, 55 and110 mm h^{-1}) were found differently. The three selected levels of the rainfall intensity factor show significant difference compared to the others (5.65m, 4.1m and 3.25m). The averages of the rill incision point of the two selected levels of the slope gradient (22 and 44%) were realized similarly as shown in Fig. 5b (4.57m vs. 4.1m). Furthermore, the interaction effects of the two factors (rainfall intensity and slope gradient) estimated in Fig. 6c shows that the averages of the rill incision point are significantly different in the slope level of 22% in the three rainfall intensities (6m , 4.05m and 3.65m). According to the figure, the averages of the rill incision point are significant in the other slope level (44%) in the three rainfall intensities (5.3, 4.15 and 2.85m). In addition, the lowest levels of intensity and slope gradient factors (10 mm/h and 22%) showed the highest interval of rill incision point until upper end flume (6 m). Thus, the highest levels of intensity and slope gradient factors show the lowest the interval rill incision point to the upper flume (2.85 meter) (Fig. 6c).

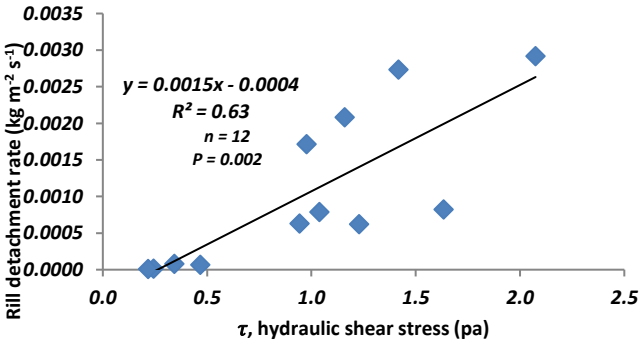


Fig. 4. Rill detachment rate on marl soil as a function of hydraulic shear stress (τ)

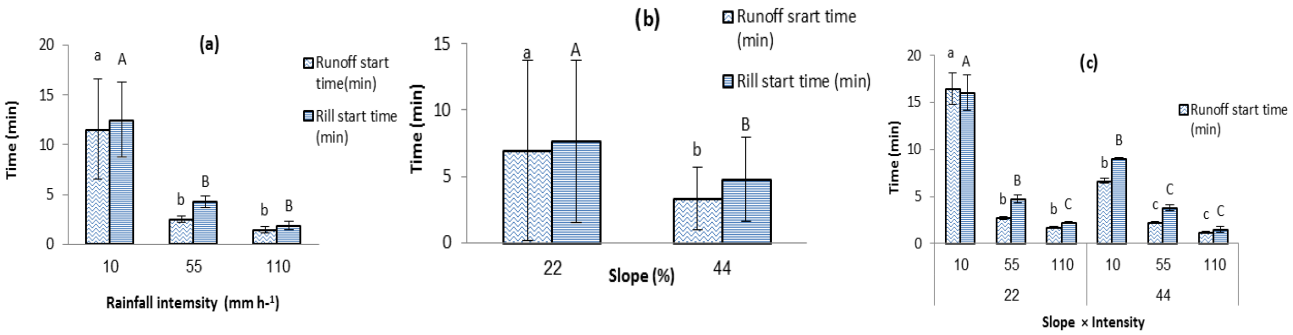


Fig.5. Runoff start time and Rill start time as a function of (a) Rainfall intensity, (b) Slope gradient and (c) Slope gradient × rainfall intensity. Common letters show non-significant mean (estimated by Tukey, P 0.05), n = 12.

Results of means comparison: Rate of soil loss

As demonstrated in Fig.7a, the averages of the rate of soil loss in the three selected levels of the rainfall intensity (10, 55 and110 mm h^{-1}) in 30 minutes rainfall, were verified differently. The highest intensity (110 mm h^{-1}) significantly shows the highest rate of soil loss compared to the two others. The three selected levels of the rainfall intensity (10, 55 and110 mm h^{-1}) were determined differently. The three selected levels of rainfall intensity factor show significant difference (0.075 kg m^{-2}, 1.29 kg m^{-2} and 4.26 kg m^{-2}). Also, the averages of the soil loss of the two selected levels of the slope (22 and 44%) were realized similar as shown in Fig. 7b. The lowest slope significantly shows the lowest soil loss compared to the other (1.55kg m^{-2} vs. 2.2 kg m^{-2}). Furthermore, the interaction effects of the two factors (rainfall intensity and slope gradient) were estimated in Fig. 7c. As shown in the figure, the averages of the soil loss are significantly different in the slope level of 44% in the three rainfall intensities (0.131 kg m^{-2}, 1.3 kg m^{-2} and 5.085 kg m^{-2}, respectively). Also, according to the figure, the averages of the soil loss are significant in the other slope level (22%) in the three rainfall intensities (0.0185 kg m^{-2}, 1.275 kg m^{-2} and 3.44 kg m^{-2}, respectively). According to the above means tests, we found out that increasing the slope gradient and rainfall intensity will induce a decrease in the runoff start time but also a decrease in the rill incision time and rill incision point. While the inverse trend can be observed as the increased soil loss (from left to right in Fig. 7c, increasing the slope gradient and rainfall intensity may lead to an increase in the soil loss. Therefore, increasing the slope gradient and rainfall intensity can direct a decrease in the runoff start time, rill incision time, and slope length of rill incision but an increase in the soil loss.

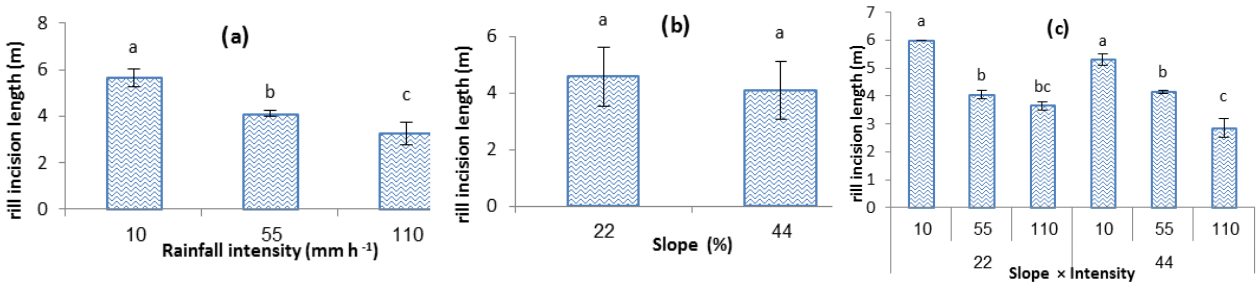


Fig.6. Rill incision point as a function of (a) Rainfall intensity, (b) Slope gradient and

(c) Slope gradient × rainfall intensity, Common letters show non-significant mean (estimated by Tukey, P≤ 0.05), n = 12.

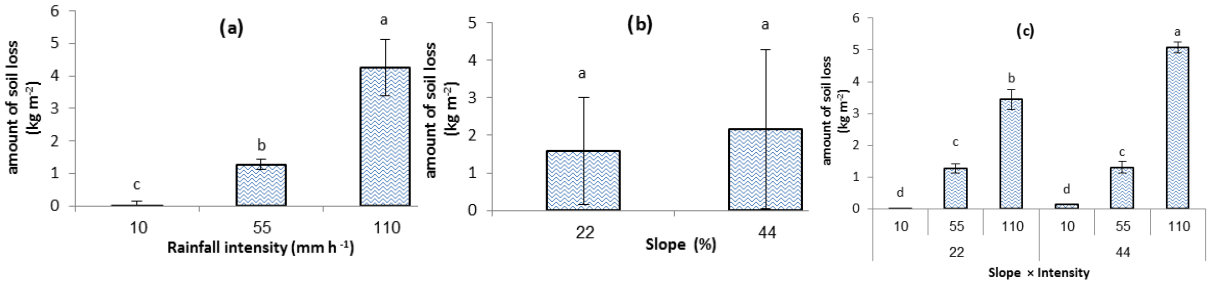


Fig.7. Soil loss as a function of (a) Rainfall intensity, (b) Slope gradient and

(c) Slope gradient × rainfall intensity; in 30 min, Common letters show non-significant mean (estimated by Tukey, P≤ 0.05), n = 12.

It can be explained that once each rill incision is formed, it will be extended to upper end of the flume. In other words, the formation of rill erosion develops with increasing the rainfall intensity and slope gradient toward upper end of the flume. During each test, the surface runoff that was available to initiate rill formation at the upstream end of the rills was limited. So the upward movement of rill head cut from the rill incision point was not significant compared with the development of the rills downslope of the point of rill initiation.

It was also determined that in the first test (i.e. rainfall intensity of 10 mm/h and slope of 22% treatment in two repetitions) did not create rill erosion during the 30 minutes precipitation. Moreover, in constant with the rainfall intensity, the increasing slope gradient will increase soil loss exponentially. As shown in Fig.7, this increasing was estimated about 6 times in low intensity (10 mm/h) and about 50 percent in high intensity (110 mm/h). According to Fig.7c, the maximum amount of the soil loss in rainfall intensity is estimated at 110 mm/h intensity whereas the minimum is 10 mm/h intensity (4.27 and 0.075 kg m^{-2} in 30 min, respectively). The results also showed that the rill incision time threshold decreases with an increase in rainfall intensity and slope gradient (Fig.7). In other words, by increasing rainfall intensity, the rill formation time reduces in relation with the start of precipitation. This means that the rills are formed in a shorter

time than before and develops toward the upside of the flume. The results of the runoff time threshold were similar to rill incision time threshold, although with different rates.

4. Discussion

The results of this study are comparable with some other investigations conducted under other conditions. For example, Yao et al. (2008) studied silty loess soils and reported a shear stress range from 1.33 to 2.63 Pa. Also, Shainberg et al., (1996) used an arable soil and determined the shear stress range from 0.79 to 1.72 Pa. Govers et al., (2007) determined the values of the soil detachment rate (per unit length) versus shear stress force (per unit length) at the slopes ranging from 0.0398 to 0.22 and discharges ranging from 5.55 (10^{-5} m^3 s^{-1}) to 6.1 (10^{-4} m^3 s^{-1}) for a silt loam soil. They also determined the shear stress and detachment rate factors' range, from 0.1 to 4.1 (kg s^{-2}) and 0 to 0.08 (kg s^{-1} m^{-1}), respectively. Persyn et al., (2005) carried out a study on the Biosolids (subsoil and top soil) which determined the shear stress range from 2.70 to 9.80 Pa for unvegetated soil and range from 4.5 to 13.00 Pa for vegetated soil. Romero et al. (2007) studied the measurement of rill erodibility factor (K_r) and concluded that K_r values can range from 0.3 to 19 × 10^{-3} s m^{-1}. Despite differences in soil type and plot size, the critical shear stress values obtained in this study were within other ranges found in other reports.

The values of marl soil erodibilty factor (K_r) and critical shear stress of marl soil Gy_1 are estimated 0.0015 s m^{-1} and 0.267 Nm^{-2}, respectively. These values are in agreement with the results of other studies such as Govers et al., (2007), Yao et al., (2008), Romero et al., (2007) and Mahmoodabadi et al., (2007). Noticeably, the parameters represent different quantities and both are needed for the measurement of erosion rates by concentrated flow in the other regions.

5. Conclusion

This paper analyzed the spatial and temporal variations of the rill formation on the hillslopes of Gy_1 marl formations that is poorly studied in Iran and available literature. The results on the rill incision (spatial and temporal) significantly demonstrated a clear downward trend of the rill incision point, runoff start time, rill start time and an upward trend of soil loss by increasing rainfall intensity and slope gradient. The study also showed a significant correlation between the rainfall intensity and slope gradient which both can affect the rill incision point, runoff start time, rill start time and the amount of soil loss. Although the rainfall intensity and slope steepness both affect the distance from the top of the plot to the point of rill initiation (slope length), rainfall intensity is found more important than the slope in the point of rill formation. In other words, the impact of rainfall intensity on the slope length of rill initiation was more significant than that of the slope. It was also proved that these parameters (slope gradient and rainfall intensity) are related with the variations of rill incision both spatially and temporary. The spatial and temporal thresholds of the rill incision have a diminishing trend with increasing slope gradient and rainfall intensity. Obviously, explaining the temporal and spatial variation in soil erosion resistance simply based on one soil property is not possible. Also, according to the measured value of marl soil erodibility, marl soil will have high sensitivity against the concentrated flows and high ability to create rill erosion on the slope ranges from 20 to 45 %. Finally, this study helps to predict and estimate the amount of soil loss per rainfall incident in a given area and also to estimate the economic value of the loss in different regions with different topography. All this can help decision makers to estimate the sustainability of a watershed more effectively.

6. Acknowledgment

The author wish to thank the Institute of Soil Conservation and Watershed Management

Research Center of Iran (ISCWM) which provided the facilities to conduct this study at the tilt flume in the simulated rainfall and erosion laboratory. Also, i wish to thank of Prof. Yan Nyssen, Prof. Frank Witlox and Dr. Hossein Azadi (Department of Geography, Gent University) for their great support during the last stages of this study.

References

1. H. Ahmadi, 1999. The applied geomorphology: water erosion vol.1, 3th ed. Tehran University, Tehran. [In Persian]
2. M. Arabkhedri, 2008. Study on Rain Characteristics and Calibration of Rainfall Simulator of Soil Conservation and Watershed Management Research Center. Final Report on 83013-0000-01-040000-003-2 Project. Institute of Soil Conservation and Watershed Management Research, Tehran. [In Persian]
3. L. Cao, K. Zhang, and W. Zhang, 2009. Detachment of road surface soil by flowing water. Catena 76, 155–162.
4. D.L. Corwin, S.M. Lesch, J.D. Oster, and S.R. Kafka, 2008. Short-term sustainability of drainage water reuse: spatio-temporal impacts on soil chemical properties. Environmental Quality 37, 8-24.
5. R.G. Foster, D.C. Flanagan, M.A. Nearing, L.J. Lane, L.M. Risse, and S.C. Finkner, 1995. Water Erosion Prediction Project (WEPP). Technical documentation. NSERL Report No.10. National Soil Erosion Research Laboratory. USDA-ARS-MWA.1196 SOIL Building. West Lafayette, IN 47907-1196.
6. G. Govers, R. Giménez, and K. Van Oost, 2007. Rill erosion: Exploring the relationship between experiment modelling and field observations. Earth Science Reviews 84, 87–102.
7. G. Govers, 1990. Empirical relationships for the transport capacity of overland flow in erosion, transport and deposition Processes. IAHS 189, 45-63.
8. G. Govers, 1992. Relationship between discharge, velocity and flow area for rills eroding loose, non-layered materials. Journal of Earth Surface Processes and Landforms 17(5), 515-528.
9. J.W Hummel, K.A. Sudduth, and S.E. Hollinger, 2001. Soil moisture and organic matter prediction of surface and subsurface soils using an NIR soil sensor. Computers and Electronics in Agriculture 32, 149–165.
10. A. Knapen, J. Poesen, G. Govers, G.Gyssels, J. Nachtergaele, 2007. Resistance of soils to concentrated flow erosion: A review. Earth Science Reviews 80, 75-109.
11. P.I.A. Kinnell, 2005. Raindrop-impact-induced erosion processes and prediction: A review. Hydrology Process 19, 2815-2844.
12. O.V. McHugh, T. Steenhuis, B. Abebe, and M. Fernandes, 2007. Performance of in situ rainwater conservation tillage techniques on dry spell mitigation and erosion control in the drought-prone North Wello zone of the Ethiopian highlands. Soil and Tillage Research 97, 19-36.
13. J. Nachtergaele, j. Poesen, 2002. Spatial and temporal variations in resistance of loess derived soils to ephemeral gully erosion. European Journal of Soil Science 53, 449–463.

14. M.A.Nearing, G.R. Foster, L.J. Lane, and S.C. Finkner, 1999. A process-based soil erosion model for USDA Water Erosion Prediction Project technology. Trans. ASAE 32(5), 1587-1593.
15. R.A. Persyn, T.D. Glanville, T.L. Richard, J.M. Laflen, and P.M.Dixon, 2005. Environmental effects of applying composted organics to new highway embankments: Part III Rill erosion. Trans ASAE 48(5), 1765-1772.
16. J. Poesen, s.F. Ingelmo and H. Mucher, 1990. The hydrological response of soil surfaces to rainfall as affected by cover and position of rock fragments in the top layer. Earth Surf Process Landforms 15, 653–671.
17. C. Romero, L. Stroosnijder, and G.A. Baigorria, 2007. Interrill and rill erodibility in the northern Andean Highlands. Catena 70, 105–113.
18. S.H. Schoenholtz, H. Van Miegroet, and J.A. Burger, 2000. A review of chemical and physical properties as indicators of forest soil quality: challenges and opportunities. Forest Ecology and Management 138, 335-356.
19. I. Shainberg, D. Goldstein, and G.J. Levy, 1996. Rill erosion dependence on soil water content, aging and temperature. Journal of SSSA 60(3), 916-922.
20. G.J. Sheridan, H.B. So, R.J. Loch, C. Pocknee, and C.M.Walker, 2000. Use of laboratory scale rill and interrill erodibility measurements for the prediction of hillslope scale erosion on rehabilitated coal mine soils and overburdens. Australian Journal of Soil Research 38, 285–297.
21. Soil Conservation and Watershed Management Research Center of Iran, 2005. The countenance of Iran's watersheds. The final report of forest range and watersheds management organization. Institute of Soil Conservation and Watershed Management Research, Tehran. [In Persian]
22. H.L. Throop, S.R. Archer, H.C. Mongerc, and S. Waltman, 2012. When bulk density methods matter: Implications for estimating soil organic carbon pools in rocky soils. Arid Environments 77, 66-71.
23. D. Torri, M. Sfalaga, and M. Del Sette, 1987. Splash detachment: Runoff depth and soil cohesion. Catena 14, 149-155.
24. T.J. Toy, G.R. Foster, and K.G. Renard, 2002. Soil erosion processes, prediction measurement under simulated rainfall. Journal of Soil Science 150, 787-798.
25. C. Yao, T. Lei, W.J. Elliot, D.K. McCool, J. Zhao, and S. Chen, 2008. Critical condition for rill initiation. Tran. ASABE 51(1), 107-114.
26. Q. Zhang, T. Lei, and J.Zhao, 2008. Estimation of the detachment rate in eroding rills in flume experiments using an REE tracing method. Geoderma 147, 8-15.